AIP | Applied Physics Letters

In-situ small-angle x-ray scattering study of nanoparticles in the plasma plume induced by pulsed laser irradiation of metallic targets

L. Lavisse, J.-L. Le Garrec, L. Hallo, J.-M. Jouvard, S. Carles et al.

Citation: Appl. Phys. Lett. **100**, 164103 (2012); doi: 10.1063/1.4703930
View online: http://dx.doi.org/10.1063/1.4703930
View Table of Contents: http://apl.aip.org/resource/1/APPLAB/v100/i16
Published by the American Institute of Physics.

In-situ small-angle x-ray scattering study of nanoparticles in the plasma plume induced by pulsed laser irradiation of metallic targets

L. Lavisse,[1,a)] J.-L. Le Garrec,[2] L. Hallo,[3] J.-M. Jouvard,[1] S. Carles,[2] J. Perez,[4] J. B. A. Mitchell,[2] J. Decloux,[5] M. Girault,[1] V. Potin,[1] H. Andrzejewski,[1] M. C. Marco de Lucas,[1] and S. Bourgeois[1]

[1]*Laboratoire Interdisciplinaire Carnot de Bourgogne (ICB), UMR 6303 CNRS-Université de Bourgogne, 9 Avenue A. Savary, BP 47870-21078 Dijon Cedex, France*
[2]*Institut de Physique de Rennes, UMR 6251 CNRS-Université de Rennes 1, 35042 Rennes Cedex, France*
[3]*CEA CESTA, 15 Avenue des Sablières CS 60001, 33116 Le Barp Cedex, France*
[4]*Synchrotron SOLEIL, L'Orme des Merisiers, Saint-Aubin, F-91192 Gif-sur-Yvette Cedex, France*
[5]*Kaluti System, Optique et Laser, Centre Scientifique d'Orsay, 91400 Orsay, France*

(Received 16 December 2011; accepted 28 March 2012; published online 16 April 2012)

Small angle x-ray scattering was used to probe *in-situ* the formation of nanoparticles in the plasma plume generated by pulsed laser irradiation of a titanium metal surface under atmospheric conditions. The size and morphology of the nanoparticles were characterized as function of laser irradiance. Two families of nanoparticles were identified with sizes on the order of 10 and 70 nm, respectively. These results were confirmed by *ex-situ* transmission electron microscopy experiments. © *2012 American Institute of Physics*. [http://dx.doi.org/10.1063/1.4703930]

Irradiation of a metallic surface by a pulsed laser source can lead to the formation of a plume for pulse durations shorter than several tens of nanoseconds.[1] Such treatments are currently used industrially for marking or cleaning metallic substrates such as iron[2] or titanium.[3] In laser ablation, the plume is essentially composed of high pressure, partially ionized plasma which expands into the ambient gas, extending typically over several millimeters and lasting some microseconds.[1,4] Pulsed laser ablation of metals gives rise to particle generation with characteristics depending on the laser fluence and the pulse duration.[5–7] Typically, for laser irradiances above 1 GW cm^{-2}, metal oxide nanoparticles are formed.[2] These nanopowders have been mostly studied by *ex-situ* electron microscopy techniques and atomic force microscopy.[5,7,8] A few *in-situ* studies of nanoparticles in the plasma plume by optical methods have been reported for the case of ultrafast (femtosecond) laser ablation of metals.[6,9,10] In the case of nanosecond laser irradiation, however, optical techniques are hindered by the presence of nanoparticles, mesoparticles, and even micro-debris in the plasma plume because the energy fluence per pulse is lower than in the femtosecond regime and thus a molten pool that ejects droplets can be formed around the irradiated zone due to thermal diffusion. Indeed, in the nanosecond laser irradiation time scale, thermal diffusion characteristic time is comparable to laser irradiation time.[8,10,11] Third generation synchrotron radiation based small angle x-ray scattering (SAXS) allows *in-situ* probing of the presence of nano and mesoparticles in such complex media to be performed. In the previous work, we have used SAXS to study particle size distributions in diffusion flames[12] and in microwave-generated fireballs.[13]

In this paper, we report recent experimental results obtained using SAXS on the SWING beamline at the SOLEIL synchrotron, where nanoparticles formed in a short-pulse laser induced plasma plume have been probed *in-situ*. In this experiment, the size and morphology of the nanoparticles formed in a titanium plasma plume have been studied as function of laser irradiance. It is worth noting that in our previous work,[12,13] it was possible to consider the system under study as being in a quasi-steady state, but this is no longer the case in the present experiment. Here, the plume is in constant expansion and the spatial and temporal time scales are very different.

In these SAXS experiments, titanium plates (commercially pure grade 4, Cezus) with dimensions of $15 \times 20 \times 1\ mm^3$ were used as targets. They were irradiated under atmospheric pressure in air by the fundamental harmonic of a Nd:YAG laser operating at 1064 nm with a full width at half maximum of 5 ns and a total Gaussian beam pulse duration of ~18 ns. The laser beam irradiance absorbed by the target material was between 0.5 and 1.2 GW cm^{-2}, the diameter of the beam on the titanium target being 110 μm. In the previous experiments with a similar laser source irradiating a titanium target in air, the general shape of the plume was found to be hemispherical, its height and width being about 2.8 and 5 mm, respectively.[1] The x-ray beam from the synchrotron (80 μm high × 300 μm wide) intersected the plume at a height of 500 μm cutting the axis of the laser beam at the center of its width (Fig. 1). The laser plume undergoes a rapid spatial expansion, which is

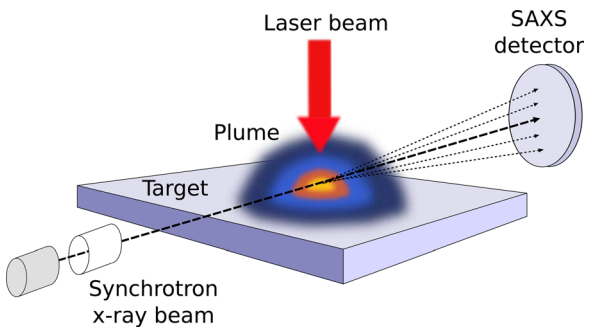

FIG. 1. Experimental setup displaying the synchrotron scattering experiment in the presence of the plume.

[a)]Electronic mail: luc.lavisse@u-bourgogne.fr.

slowed down due to its compression in the ambient air. Its velocity along the axis of the incident laser beam, calculated under similar thermodynamic and material conditions, is about 10^5 m/s.[14] This is considerably lower than that reached when the plume expands freely into vacuum. Thus, the time needed for the ablated material coming from the target to reach a height of 500 μm is about 5 ns. According to numerical simulations of laser irradiated targets and subsequent hydrodynamic processes,[11,15,16] this time corresponds approximately to the time necessary for the formation of nanopowders.

The energy of the x-rays was chosen to be 9 keV to reduce absorption by the ambient air and the detector was positioned at 3 m from the target plume. In this configuration, the measured scattering vector, $q = (4\pi/\lambda)\sin(\theta/2)$, where λ and θ are the wavelength of the incident x-ray radiation and the scattering angle, respectively, covers the range from 0.002 to 0.3 Å^{-1}. Fig. 2 shows a typical background subtracted scattering intensity, $I(q)$, as a function of the scattering vector q. Since above $q \sim 0.05$ Å^{-1}, $I(q)$ tends towards zero, the useful q range was in fact between 0.002 and 0.05 Å^{-1}. Since the particle size can be approximately estimated by the expression $D = \pi/q$, our measurements could detect particles with a range of sizes typically from 6 to 170 nm.

Background scattering intensity in air was first recorded without any laser firing. Then, for each laser irradiance, i.e., laser repetition rate (see Table I), at least 20 measurements, with 1 s acquisition time, were performed in a row without interrupting the laser. In order to obtain sufficient scattering signal intensity, a 1 s acquisition time was necessary to build up sufficient particle density although each individual plume lasts only for a few microseconds.[14] Due to the high repetition rate of the laser, the density of particles from one plume adds to the decaying plume from the previous shot, thus, producing a cloud of particles. As a consequence, it was not possible to spatially map the plume, the scattering signal being an average of many shots corresponding to the repetition rate (for example, 1 s acquisition time at 75 kHz laser repetition rate induces a cumulated scattering intensity over 75 000 plumes).

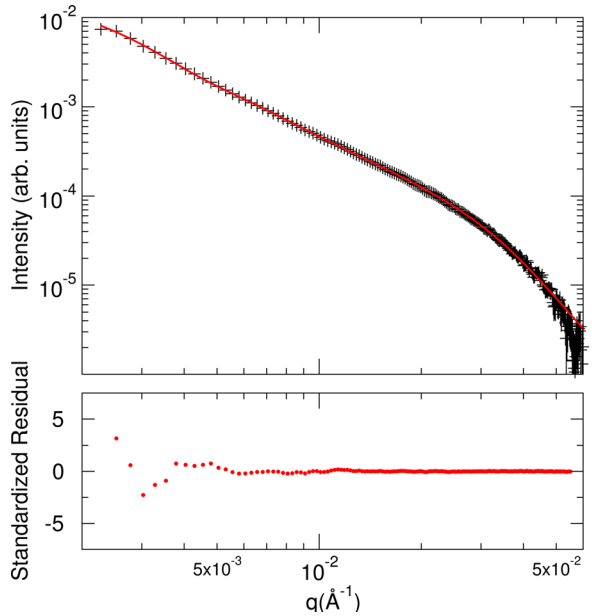

FIG. 2. Typical SAXS intensity, $I(q)$, as a function of scattering vector q obtained with a 20 kHz repetition rate of the laser. The experimental intensity (+) is fitted (—) using the two levels unified exponential/power-law function (see Ref. 18).

TABLE I. Evolution of the radius of gyration R_g and of the Porod index P versus the irradiance of the laser. R_g and P have been determined from the analysis of the background subtracted scattering intensity for the overall $(R_{g,1}, P_1)$ and the substructure $(R_{g,2}, P_2)$ particles. These values are the average of 20 measurements.

Laser		Particles			
Parameters		Overall		Substructure	
Repetition rate (kHz)	Irradiance (GW cm^{-2})	$R_{g,1}$ (nm)	P_1	$R_{g,2}$ (nm)	P_2
20	1.2	74	2.1	6.7	4.0
50	0.75	66	2.1	8.0	4.0
75	0.5	55	1.9	16.0	4.0

Analysis of the scattering pattern has been performed using the two level Beaucage unified exponential/power-law fitting function[17]

$$I(q) = G_1\exp\left(-\frac{q^2R_{g,1}^2}{3}\right) + G_2\exp\left(-\frac{q^2R_{g,2}^2}{3}\right) + B_1\exp\left(-\frac{q^2R_{sub}^2}{3}\right)\left\{q^{-1}\left[\mathrm{erf}\left(\frac{qR_{g,1}}{\sqrt{6}}\right)\right]^3\right\}^{P_1} + B_2\left\{q^{-1}\left[\mathrm{erf}\left(\frac{qR_{g,2}}{\sqrt{6}}\right)\right]^3\right\}^{P_2}. \quad (1)$$

This unified function describes the scattering of particles which contain multiple levels of related structural features and can be applied to a wide variety of systems, such as polydisperse mass fractal, surface fractal, and diffuse surface particles. Basically, each structural level is represented, in its particular range of q values, by a Guinier exponential form at low q and an associated power-law in the high q range; the so-called Porod region. The subscripts 1 and 2 refer to larger and smaller structural features, respectively. R_g denotes the radius of gyration and R_{sub} denotes the high-q cut-off for the power-law describing the mass-fractal regime, whose low q limit is at $R_{g,1}$. For fractals, R_{sub} is usually equal to the substructure radius of gyration, $R_{g,2}$. G, B, and P are the exponential pre-factor, the constant pre-factor specific to the type of power-law scattering, and the power-law exponent associated with each structural level, respectively. To fit this equation to our data, the small angle scattering (SAS) macro package from Ilavsky of the Advanced Photon Source has been used.[18] In the present case, all the background subtracted scattering x-ray intensities were fitted using a two-level function. Typical experimental data and the corresponding fitted curve are shown in Fig. 2. The goodness of fit is determined by calculating the standardized residual and this is also shown in Fig. 2. It should be noted that a single family fit to the data yields much larger standardized residuals and this gives us confidence in attributing the data to two families.

Each individual background subtracted scattering intensity is analysed as mentioned above, and the averaged values of the radii of gyration for both the smaller and larger particles are shown in Table I as a function of the irradiance of the laser. It has to be noted that when the repetition rate of the laser increases, its irradiance decreases as already demonstrated for such a laser source.[8] The smallest detected particles having radii of gyration of the order of 7 nm increase slightly in size when the irradiance laser decreases. The average power-law exponent (Porod index) has also been evaluated and a value of 4 for these smaller particles has been found, independent of the irradiance of the laser. This means that these particles have a smooth surface and the transition between the particle and the surrounding medium is sharp.[12,19] For the larger particles, the radii of gyration increases from 55 nm at 0.5 GW cm^{-2} to 75 nm at 1.2 GW cm^{-2}. The value of the Porod index obtained close to 2 indicates that the scatterer is a Gaussian polymer chain which is consistent with an agglomeration of smaller particles.[19] These *in-situ* observations can be explained qualitatively by modelling based on the thermodynamic path of the plasma.[20] Given the height of the observation (500 μm), one should observe small particles in the core and large ones at the periphery.

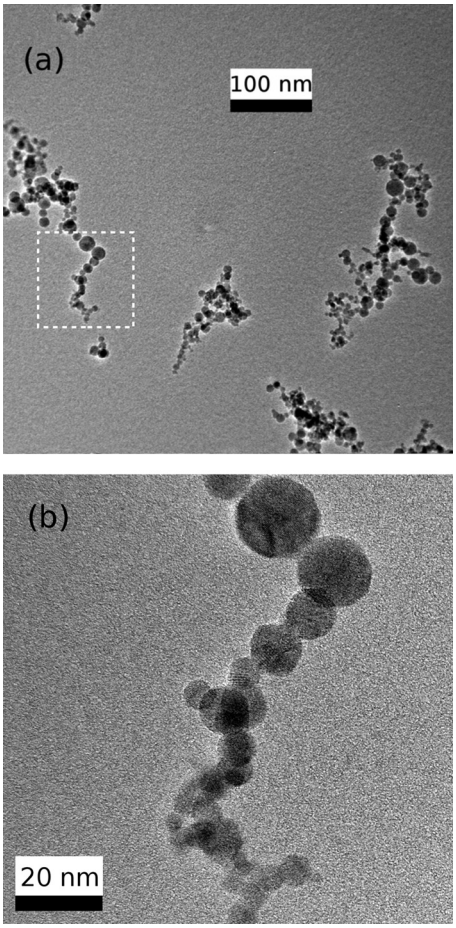

FIG. 3. TEM images of nano-powders obtained by pulsed laser irradiation of a Ti target. (a) General view of nanoparticles showing necklace organization. (b) Zoom evidencing nanoparticles of about 10 nm in size.

In order to complete this study, *ex-situ* conventional transmission electron microscopy analyses of powders deposited on a sampling plate during the pulsed laser irradiation of the target have been made with a 200 kV JEOL 2100 (LaB_6) microscope. Fig. 3(a) shows a general view of the collected particles displaying a necklace type organisation. Fig. 3(b) shows that the size of the individual particles as well as the observed smooth and sharp interface with the medium are consistent with SAXS results.

In conclusion, we report here SAXS measurements performed on a plasma plume generated by a pulsed laser on a titanium target, demonstrating the existence of at least two families of nanoparticles. The smallest, with radii of gyrations of about 10 nm, grow in the plume by condensation and then aggregate to form structures in the form of a necklace of about 55–75 nm in size, depending upon the irradiance of the laser. Modelling based on saturation and condensation processes in the plume is now in progress allowing realistic thermodynamic paths to be obtained, which can explain the formation and also the size of these particles.

The authors would like to thank synchrotron SOLEIL for experimental and financial assistance with this project. Thanks are also due to the CNRS Plasmas Froids network programme that led to the initiation and financing of this collaborative effort.

[1]L. Lavisse, P. Berger, M. Cirisan, J. M. Jouvard, S. Bourgeois, and M. C. Marco de Lucas, J. Phys. D: Appl. Phys. **42**, 245303 (2009).
[2]A. Pereira, A. Cros, P. Delaporte, W. Marine, and M. Sentis, Appl. Surf. Sci. **208**, 417 (2003).
[3]A. P. del Pino, P. Serra, and J. L. Morenza, Thin Solid Films **415**, 201 (2002).
[4]D. Blair, M. Tillack, and M. Zaghloul, Proc. SPIE **4557**, 139 (2001).
[5]B. Liu, Z. Hu, Y. Che, Y. Chen, and X. Pan, Appl. Phys. Lett. **90**, 044103 (2007).
[6]D. B. Geohegan, A. A. Puretzky, and D. J. Rader, Appl. Phys. Lett. **74**, 3788 (1999).
[7]S. H. Ko, Y. Choi, D. J. Hwang, C. P. Grigoropoulos, J. Chung, and D. Poulikakos, Appl. Phys. Lett. **89**, 141126 (2006).
[8]I. Shupyk, L. Lavisse, J. M. Jouvard, M. C. Marco de Lucas, S. Bourgeois, F. Herbst, J. Piquemal, F. Bozon-Verduraz, and M. Pilloz, Appl. Surf. Sci. **255**, 5574 (2009).
[9]F. R. A. Onofri, M. Wozniak, and S. Barbosa, Contrib. Plasma Phys. **51**, 229 (2011).
[10]D. B. Geohegan, A. A. Puretzky, G. Duscher, and S. Pennycook, Appl. Phys. Lett. **72**, 2987 (1998).
[11]E. Lescoute, L. Hallo, B. Chimier, D. Hebert, V. T. Tikhonchuk, C. Stenz, J. M. Chevalier, J. L. Rullier, and S. Palmier, Eur. Phys. J. Spec. Top. **175**, 159 (2009).
[12]J. B. A. Mitchell, S. di Stasio, J. L. Le Garrec, A. I. Florescu-Mitchell, T. Narayanan, and M. Sztucki, J. Appl. Phys. **105**, 124904 (2009).
[13]E. Jerby, A. Golts, Y. Shamir, S. Wonde, J. B. A. Mitchell, J. L. Le Garrec, T. Narayanan, M. Sztucki, D. Ashkenazi, Z. Barkay, and N. Eliaz, Appl. Phys. Lett. **95**, 191501 (2009).
[14]M. Cirisan, J. M. Jouvard, L. Lavisse, L. Hallo, and R. Oltra, J. Appl. Phys. **109**, 103301 (2011).
[15]J. Breil, S. Galera, and P. H. Maire, Comput. Fluids **46**, 161 (2011).
[16]J. P. Colombier, P. Combis, F. Bonneau, R. Le Harzic, and E. Audouard, Phys. Rev. B **71**, 165406 (2005).
[17]G. Beaucage, J. Appl. Cryst. **28**, 717 (1995).
[18]J. Ilavsky and P. R. Jemian, J. Appl. Cryst. **42**, 347 (2009).
[19]T. Narayanan, in *Applications of Synchrotron Light to Scattering and Diffraction in Materials and Life Sciences*, edited by M. Gomez, A. Nogales, M. C. Garcia-Gutierrez, and T. A. Ezquerra (Springer, Berlin, 2009), Vol. 776, p. 133.
[20]B. Chimier, V. T. Tikhonchuk, and L. Hallo, Phys. Rev. B **75**, 195124 (2007).